



## RESEARCH ARTICLE

10.1029/2018MS001447

## Special Section:

The Max Planck Institute for Meteorology Earth System Model version 1.2

## Key Points:

- In MPI-ESM, the AMOC strength strongly declines with enhanced atmospheric resolution
- This is due to freshening of the North Atlantic caused indirectly by weaker winds that reduce wind-driven gyre and salinity transport into the region
- We use a lower-resolution setup to mimic higher-resolution runs by implementing surface flux correction and thus reduce computational cost by 75%

## Correspondence to:

D. A. Putrasahan,  
dian.putrasahan@mpimet.mpg.de

## Citation:

Putrasahan, D. A., Lohmann, K., von Storch, J.-S., Jungclaus, J. H., Gutjahr, O., & Haak, H. (2019). Surface flux drivers for the slowdown of the Atlantic Meridional Overturning Circulation in a high-resolution global coupled climate model. *Journal of Advances in Modeling Earth Systems*, 11. <https://doi.org/10.1029/2018MS001447>

Received 18 JUL 2018

Accepted 12 MAR 2019

©2019. The Authors.

This is an open access article under the terms of the Creative Commons Attribution-NonCommercial-NoDerivs License, which permits use and distribution in any medium, provided the original work is properly cited, the use is non-commercial and no modifications or adaptations are made.

# Surface Flux Drivers for the Slowdown of the Atlantic Meridional Overturning Circulation in a High-Resolution Global Coupled Climate Model

D. A. Putrasahan<sup>1</sup> , K. Lohmann<sup>1</sup> , J.-S. von Storch<sup>1</sup> , J. H. Jungclaus<sup>1</sup> , O. Gutjahr<sup>1</sup> , and H. Haak<sup>1</sup> <sup>1</sup>Max Planck Institute for Meteorology, Hamburg, Germany

**Abstract** This paper investigates the causation for the decline of the Atlantic Meridional Overturning Circulation (AMOC) from approximately 17 Sv to about 9 Sv, when the atmospheric resolution of the Max Planck Institute-Earth System Model is enhanced from  $\sim 1^\circ$  to  $\sim 0.5^\circ$ . The results show that the slowdown of the AMOC is caused by the cessation of deep convection. In most modeling studies, this is thought to be controlled by buoyancy fluxes in the convective regions, for example, by surface freshwater flux that is introduced locally or via enormous input from glacier or iceberg melts. While we find that freshwater is still the key to the reduction of AMOC seen in the higher-resolution run, the freshening of the North Atlantic does not need to be directly caused by local freshwater fluxes. Instead, it can be caused indirectly through winds via a reduced wind-driven gyre circulation and salinity transport associated to this circulation, as seen in the higher-resolution run.

## 1. Introduction

Currently, the modeling community has been moving towards the use of higher-resolution global coupled climate models (Haarsma et al., 2016), with the expectation that this provides improved representation of features and processes in the climate system and reduces model biases compared to current generation models, such as the Coupled Model Intercomparison Project, Fifth phase models (Taylor et al., 2012). However, high-resolution global coupled climate models also encounter many challenges. On the technical side, high computational costs prevent extensive tuning and spin-up simulations. In addition, much is still unclear about the quantitative benefits or drawbacks from enhanced resolution. For example, Bryan et al. (2006) found increasing Atlantic Meridional Overturning Circulation (AMOC) strength with enhanced atmosphere model resolution in the Community Climate System Model. However, using simulations with the high-resolution Max Planck Institute for Meteorology Earth System Model (MPI-ESM), we find that the AMOC strength strongly declines with enhanced atmospheric resolution. Even with model biases such as the cold and fresh bias in the North Atlantic, climate variability and predictability studies can still be conducted (Menary et al., 2015; Pohlmann et al., 2004; Weijer et al., 2012a). However, cold and fresh waters in the North Atlantic that develop with a slowdown in the AMOC can have severe climate change implications. Hence, the goal of this paper is to understand this resolution-dependent behavior of the AMOC.

The AMOC is composed of an upper warm water branch flowing northward that is compensated by a colder southward returning branch at depth. At high latitudes, heat loss to the atmosphere cools the northward flowing salty surface water, making it cold and dense and thus causing it to sink into the deep ocean, where it connects to the returning branch (see detailed reviews on the AMOC by Buckley & Marshall, 2016; Kuhlbrodt et al., 2007). This deep convection occurs mostly in the Labrador and Greenland-Iceland-Norwegian Seas. If deep convection is inhibited, AMOC would slow down. Recent work has also shown that the link between deep convection and the AMOC is not necessarily simple and is mediated by the boundaries (Katsman et al., 2018).

Deep convection, which is primarily buoyancy driven, can be suppressed either by a large reduction in heat loss or if the surface waters become too fresh. A reduction in heat loss can be caused by the presence of sea ice that would insulate the ocean from the atmosphere. Too fresh waters can result from either local

or remote effects. For example, melt water from the Greenland ice sheet can cause an abrupt freshening of the surface waters (Weijer et al., 2012b). If the surface waters become too fresh, cooling surface waters would not make it dense enough to sink, thus abating deep convection and reducing the AMOC, which in turn transports less salt poleward and further decreases salinity and density in the sinking region, thereby providing a positive feedback (the salinity-advection feedback; Stommel, 1961).

The slowdown of AMOC during Heinrich events is seen through reconstruction from proxies (Bond et al., 1992; Clark et al., 2002) and has been emulated in models through “hosing” experiments (Gent, 2018; Manabe & Stouffer, 1999; Mecking et al., 2016; Rahmstorf et al., 2005), in which the North Atlantic receives a large freshwater input. Particularly in models, salinity has been shown to play a major role in modulating deep convection. Previous studies indicate the prominence of surface heat flux in reducing heat loss and surface freshwater flux in freshening the North Atlantic, which subsequently inhibited deep convection and led to the decline of the AMOC (Dixon et al., 1999; Gregory et al., 2005; Manabe & Stouffer, 1999; Mikolajewicz & Voss, 2000; Polo et al., 2014; Rahmstorf, 1996). However, changes in surface wind stress were either neglected or showed negligible effects (Dixon et al., 1999; Gregory et al., 2005). Yet other studies have shown the influence of winds on the AMOC on subseasonal to interannual time scales (Elipot et al., 2017; Ezer, 2015; Polo et al., 2014; Roberts et al., 2013; Zhao & Johns, 2014), as well as during past glacier climate periods (Klockmann et al., 2016; Zhang et al., 2014).

In this study, we reinvestigate the various factors that contribute to the salinity-advection feedback, including the possible impacts from momentum flux, in order to understand the dynamical and mechanical reasons underlying the substantial decline in the AMOC seen in our simulations. Since the same ocean resolution is used for our low- and high-resolution experiments, we hypothesize that the AMOC decline is related to atmospheric resolution-induced changes in air-sea fluxes, such as surface wind stress, heat, and freshwater fluxes. We disentangle the role of buoyancy and momentum fluxes by means of sensitivity experiments with adjusted coupling fluxes between atmosphere and ocean. Additionally, both local and remote effects of these fluxes on the density in deep convection regions are taken into account. We aim to answer the following scientific questions: (1) Which flux is most crucial for the AMOC decline? (2) How does wind stress affect the AMOC? From a computational point of view, the cost of running high-resolution sensitivity experiments is extremely expensive. Therefore, we introduce a strategy that uses lower-resolution simulations to mimic high-resolution runs, thereby cutting computational expenses by about 75%. The paper is outlined as follows: section 2 provides model configuration and sensitivity experiments; section 3 addresses the two scientific questions; section 4 discusses other possibilities of AMOC slowdown and provides a summary of the paper.

## 2. Model Configuration and Sensitivity Experiments

MPI-ESM comprises the atmospheric general circulation model ECHAM6 (Stevens et al., 2013), the land vegetation model JSBACH (Reick et al., 2013), the ocean and sea ice model MPIOM (Jungclaus et al., 2013), the ocean biogeochemistry model HAMOCC (Ilyina et al., 2013), and the OASIS coupler (Valcke, 2013) to exchange flux information between the atmosphere and ocean. MPI contributes to the High Resolution Intercomparison Project (HighResMIP; Haarsma et al., 2016) by providing global coupled climate simulations with varying horizontal resolutions that are higher than the standard resolution in Coupled Model Intercomparison Project-Phase 6 (CMIP6; Eyring et al., 2016). Among the MPI-ESM model (Mauritsen et al., 2012) configurations that are used in CMIP6, the highest standard resolution (Müller et al., 2018) uses a  $0.4^\circ$  ocean resolution with 40 vertical levels (TP04L40, tripolar grid) with a  $1^\circ$  atmosphere (T127 spectral model with 95 vertical hybrid levels). This setup corresponds to the low-resolution setup for HighResMIP and is denoted as HR based on resolution naming convention within MPI-ESM CMIP6 simulations. The high-resolution MPI-ESM setup for HighResMIP is called XR and utilizes the same  $0.4^\circ$  ocean resolution as HR but with an increased atmospheric resolution of T255 ( $0.5^\circ$  with 95 vertical hybrid levels). We denote the control HR and XR simulations as HR<sub>orig</sub> and XR<sub>orig</sub>, respectively. HR<sub>orig</sub> is 100 years of a control simulation taken from an equilibrated, multicentennial, preindustrial 1850 run. XR<sub>orig</sub> is a 150-year control simulation initialized with the same ocean state and runs under the same preindustrial forcing as HR<sub>orig</sub>.

We seek to understand why in MPI-ESM, the AMOC strength achieved at an equilibrium state comparable to observations in HR would slow down by almost 50% when the atmospheric resolution is doubled to XR (Figure 1). The only difference between these runs arises from atmospheric resolution differences, which

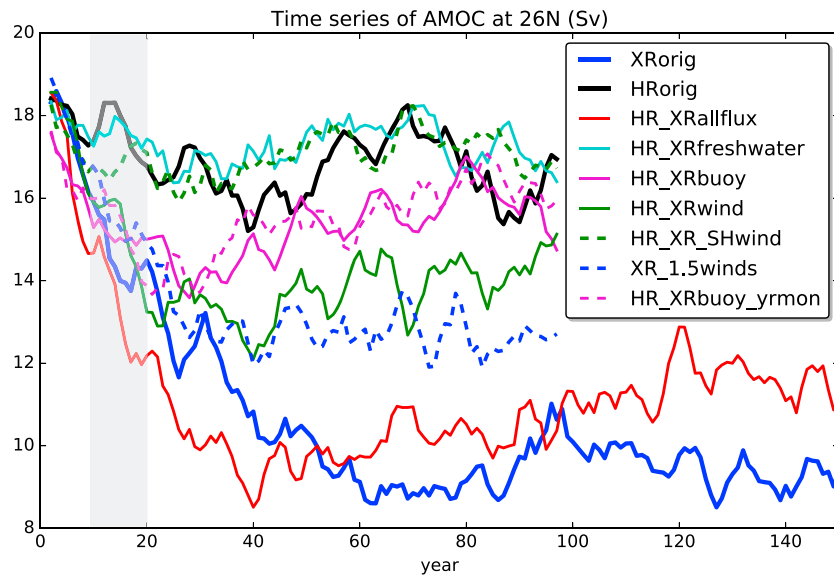


**Figure 1.** Five-year running mean of AMOC strength (Sv) at 26°N, 1,000-m depth in various model experiments as listed in the Table 1. Analysis window for sea ice extent and mixed layer depth calculations used in Figures 2, 5, 6, and 9 is marked in gray. AMOC = Atlantic Meridional Overturning Circulation.

would induce surface flux differences that are expected to either directly or indirectly affect the AMOC. Hence, we conduct a series of simulations (listed in Table 1) to test the sensitivity of AMOC to surface flux differences induced by the increased atmospheric resolution and disentangle their individual contributions. As we increased the atmospheric resolution from T127 to T255, we did not change any atmospheric parameters except for the horizontal diffusion damping term. This is done so that we can assess the impact of resolution on the decline of the AMOC without added complications that may arise due to changes in atmospheric parameters. Similarly, the coupling time step is set to the ocean time step, which is hourly and the same for all sensitivity experiments. However, the atmospheric time step is decreased from 200 s in HR to 90 s in XR so as to keep the model integration stable. It should be noted that the computational expense for such sensitivity experiments with XR is very expensive; hence, we adopt a strategy that uses the HR configuration to mimic XR simulations by implementing a surface flux correction at every coupling step. While flux correction is a common practice for sensitivity studies, this is, to our knowledge, the first time flux corrections to a different resolution is used in a coupled setup. Being able to use HR-corrected runs to emulate XR simulations allows us to reduce computational resources by about a factor of 4.

Here, we define the flux correction,  $\Delta F$ , as a difference in the fluxes of the first 20-year mean climatology of XRorig and HRorig runs, that is,  $\Delta F = \bar{F}_{XRorig} - \bar{F}_{HRorig}$ , where overbar indicates time mean. The time mean of the first 20 years is chosen since the steep decline in AMOC is seen within this period and we aim to understand the processes occurring during this steep decline. Reynolds decomposition can be applied to

**Table 1**  
*List of Sensitivity Experiments Conducted*

| Experiment name    | Description  |
|--------------------|--|
| HRorig (T127/TP04) | Control run at low resolution (preindustrial)              |
| XRorig (T255/TP04) | Control run at high resolution (preindustrial)             |
| HR_XRallflux       | Momentum, freshwater, and heat fluxes adjusted to XR       |
| HR_XRfreshwater    | Only freshwater flux adjusted to XR                        |
| HR_XRbuoy          | Only freshwater and heat fluxes adjusted to XR             |
| HR_XRwind          | Only wind stress adjusted to XR                            |
| HR_XR_SHwind       | Only wind stress in the Southern Hemisphere adjusted to XR |
| XR_1.5winds        | XR with 1.5* (wind stress)                                 |

the fluxes of each run such that the flux, in for instance HRorig, can be represented as

$$F_{\text{HRorig}} = \bar{F}_{\text{HRorig}} + F'_{\text{HRorig}}$$

where ' indicates deviations from the time mean. The flux in a HR simulation that mimics flux from XR can then be written as

$$\begin{aligned} F_{\text{HR\_XRept}} &= F_{\text{HR\_XRept\_atm}} + \Delta F \\ &= \bar{F}_{\text{HR\_XRept\_atm}} + F'_{\text{HR\_XRept\_atm}} + \bar{F}_{\text{XRorig}} - \bar{F}_{\text{HRorig}} \\ &\approx \bar{F}_{\text{XRorig}} + F'_{\text{HR\_XRept\_atm}} \end{aligned}$$

where HR\_XRept are the various sensitivity experiments that use HR configuration with corrections to XR fluxes (Table 1). For instance, we have a 150-year simulation at HR resolution with corrections to all XR mean surface fluxes that is called HR\_XRallflux.  $F_{\text{HR\_XRept}}$  are the surface fluxes that the ocean component from each HR\_XRept experiment sees, while  $F_{\text{HR\_XRept\_atm}}$  are the surface fluxes that the atmospheric component produces. Here, we expect that the fluxes we change play a major role relative to those unchanged, such that we assume the time means for all HR runs in the first few decades are equal, that is,  $\bar{F}_{\text{HR\_XRept\_atm}} = \bar{F}_{\text{HRorig}}$ , and that imposing a flux correction on a HR simulation provides a corrected simulation that employs the mean fluxes of XR but retains variability from HR. Initially, differences in the unchanged fluxes between  $\bar{F}_{\text{HR\_XRept\_atm}}$  and  $\bar{F}_{\text{HRorig}}$  are small compared to differences between  $\bar{F}_{\text{XRorig}}$  and  $\bar{F}_{\text{HRorig}}$ . However, because it is a coupled system, providing a perfectly *correct* flux correction is problematic due to circulation changes, sea ice formation, and feedbacks that occur (Gregory et al., 2016) and evolve with increasing time, leading to changes in untouched fluxes with time. In our study, the focus is on the transient decline of the AMOC in the first few decades, for which our assumption holds.

From this framework, we are able to investigate the role of all coupling fluxes simultaneously or individually. For example, the flux corrected to the wind stress from XR can be applied without affecting the buoyancy flux exchange which also depends on wind (HR\_XRwind in Table 1). This allows us to explicitly study the role of wind stress on the salinity-advection feedback. Since previous studies emphasized the importance of local buoyancy fluxes, and particularly freshwater flux, to the slowdown of the AMOC, we performed separate runs for buoyancy flux correction (heat + freshwater; HR\_XRbuoy) and for explicit freshwater correction (HR\_XRfreshwater). Each component-wise flux-corrected runs are 100 years long and are initialized from the same state as HRorig.

Other types of flux correction can be implemented. Regional corrections to the fluxes can be implemented, for example, by imposing only Southern Hemispheric wind stress from XR (HR\_XR\_SHwind in Table 1). Flux correction can also include multiplying a factor to its mean state, allowing us to assess the impact of an increased mean flux without explicitly touching its variability. This is done in experiment XR\_1.5winds (Table 1), where mean wind stress is increased by a factor of 1.5. In this case, the flux correction is defined by  $\Delta\tau = 0.5 \times \bar{\tau}_{\text{XRorig}}$ , and the actual wind stress used is modified accordingly as

$$\begin{aligned} \tau_{\text{XR\_1.5winds}} &= \tau_{\text{XRorig}} + \Delta\tau \\ &= \bar{\tau}_{\text{XRorig}} + \tau'_{\text{XRorig}} + 0.5 \times \bar{\tau}_{\text{XRorig}} \\ &= 1.5 \times \bar{\tau}_{\text{XRorig}} + \tau'_{\text{XRorig}} \end{aligned}$$

where overbars are time means and ' are deviations from the time mean. In this case, XR configuration is used rather than HR. Here, XR\_1.5winds is a 100-year simulation that uses the same initialization as XRorig.

### 3. Results

#### 3.1. Impact of Atmospheric Resolution-Induced Surface Flux Differences on AMOC

The AMOC in MPI-ESM is primarily affected by salinity-driven deep convection in the Labrador Sea and Greenland-Iceland-Norwegian seas. The lower-resolution MPI-ESM (denoted as HR) produces an AMOC at 26°N of about 17 Sv, while the higher-resolution MPI-ESM (denoted as XR) produces an AMOC at 26°N that equilibrates at approximately 9 Sv (Figure 1). The same can be inferred from AMOC time series at 45°N (not shown). This weakening of the AMOC in XR is manifested through the formation of sea ice and complete shutdown of subpolar deep convection in the Labrador Sea (Figures 2a and 2b). In this study, mixed layer depth is used as a proxy for deep convection, and is defined as the depth at which the difference in

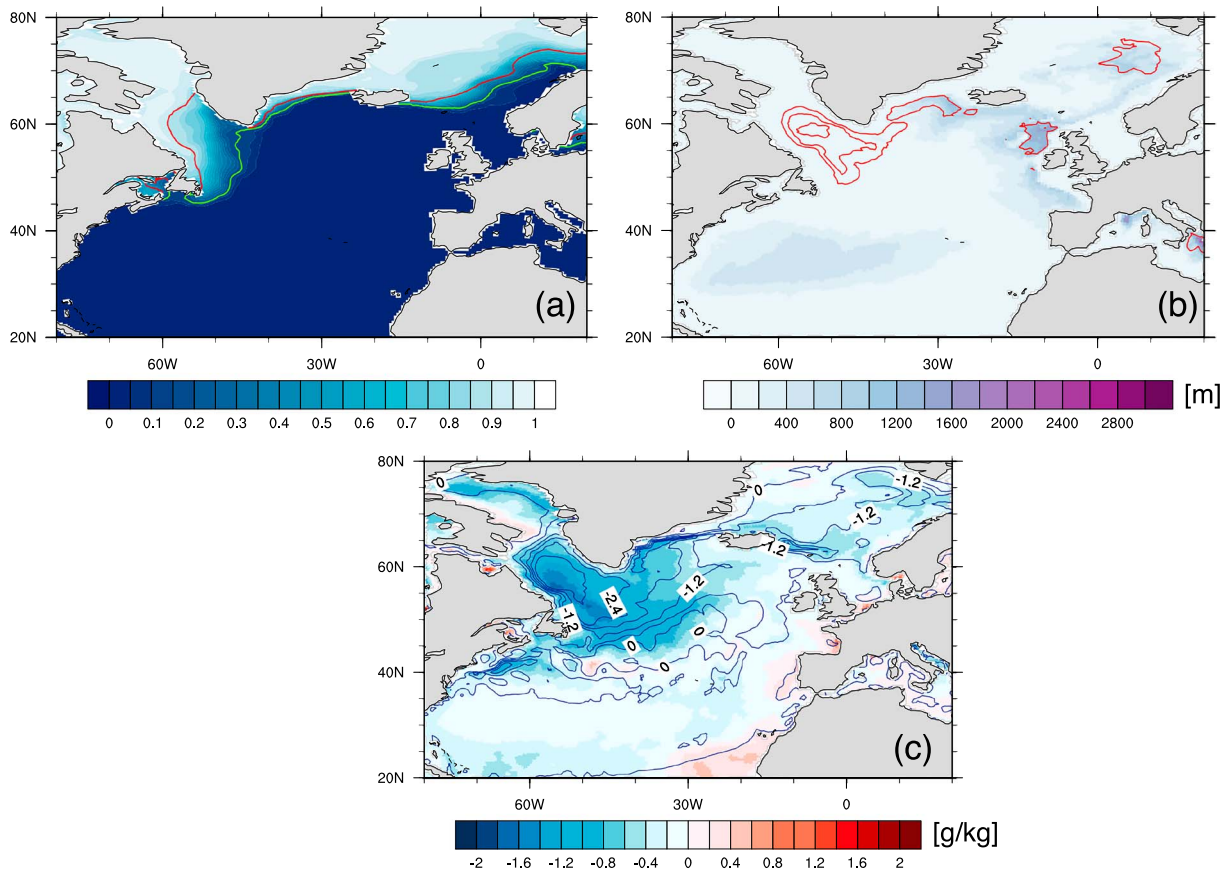


**Figure 2.** (a) Mean sea ice fraction in March for the second decade of XRorig in color. Red line represents the extent of 0.15 sea ice fraction for HRorig and green line for XRorig. (b) Mean mixed layer depth (m) in March for the second decade of XRorig in color. Red lines are 1,000-, 2,000-, and 3,000-m mixed layer depth contours from HRorig. (c) Mean difference of the first 20 years of (XRorig – HRorig) for sea surface salinity (psu) in color and sea surface temperature (contours at 0.6 °C interval).

density relative to surface density is  $0.125 \text{ kg/m}^3$ . Reduction of the AMOC is also associated with cooling and freshening in the subpolar North Atlantic (Figure 2c). Since an identical ocean model configuration is used in HR and XR, the reduced AMOC in XR has to be attributed to atmospheric resolution-induced differences in surface freshwater, heat, and momentum fluxes. Locally enhanced freshwater flux in XR compared to HR (Figure 3a) directly freshens the western subpolar North Atlantic. Analysis of individual components of surface fresh water flux suggests that enhanced fresh water input in XR is mainly due to reduced evaporation (not shown). The formation and presence of sea ice over the Labrador Sea (Figure 2a) diminishes heat loss to the atmosphere in XR (Figure 3b), especially during boreal winter, as well as decouples the deep ocean from the surface and thus weakens deep convection (Figure 2b). Although XR produces stronger mean tropospheric jets (not shown), the surface wind stress expression is globally weaker, especially over the Southern Ocean and North Atlantic between 40° and 60°N (Figure 3c). Reduced surface winds over the North Atlantic will not only affect surface buoyancy fluxes but may also limit the lateral advection of warm and saline subtropical water by slowing down the wind-driven part of the North Atlantic ocean circulation.

### 3.2. Which Flux(es) is Most Crucial for the AMOC Decline?

We assess the various contributions of atmospheric resolution-induced surface flux changes by conducting the sensitivity experiments listed in Table 1 to determine which fluxes are important for the state of the subpolar North Atlantic and the AMOC decline in XR. In the first case, all surface fluxes are adjusted to the mean XR state. This experiment (HR\_XRallflux) is designed to check the viability of reproducing the XR simulation using the HR model. It produces a slowdown of the AMOC to about 10 Sv (red line in Figure 1), which is akin to the original XR run (XRorig; bold blue line in Figure 1), and no recovery of the AMOC is seen even as HR\_XRallflux was extended up to 200 years (not shown). In addition, as with XRorig, we find that HR\_XRallflux shows a similar cooling and freshening of the North Atlantic (Figure 4a), similar

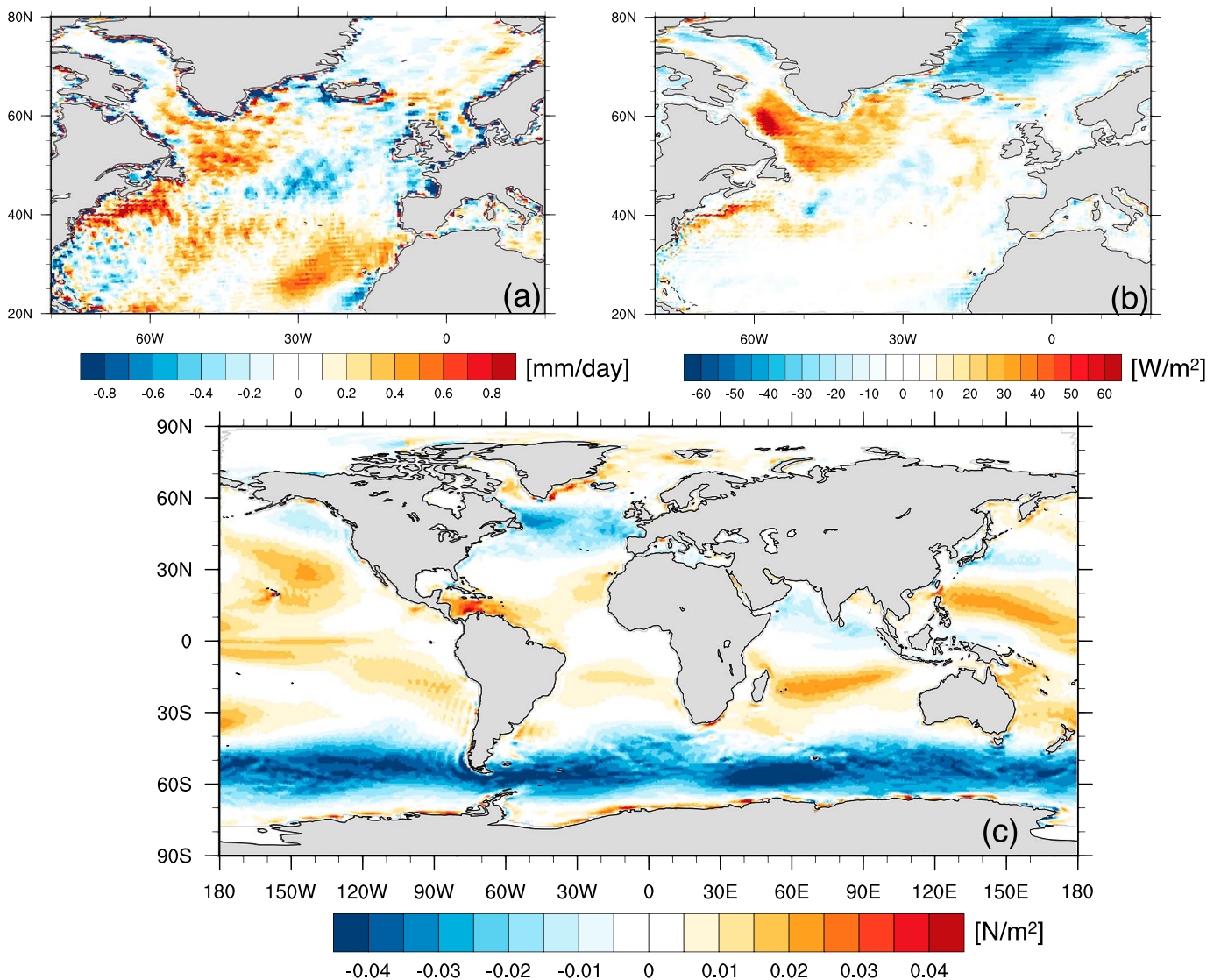


**Figure 3.** Mean difference of the first 20 years of (XRorig – HRorig) for (a) net surface freshwater flux (mm/day); (b) net surface heat flux (W/m<sup>2</sup>); and (c) zonal wind stress (N/m<sup>2</sup>). Surface fluxes are defined positive into the ocean.

sea ice extent (Figure 5a vs. Figure 2a) and a complete shutdown of the subpolar deep convection in the Labrador Sea (Figure 6a vs. Figure 2b). This supports the viability of the proposed framework to represent XR simulations with the HR configuration.

We then apply this technique individually to freshwater flux, buoyancy (heat + freshwater) flux, and wind stress over water (Table 1), to separate the buoyancy versus dynamical wind effect over the North Atlantic and on the AMOC. The freshwater flux correction in HR\_XRfreshwater alone makes negligible differences in AMOC (cyan and black lines in Figure 1). Surface salinity and temperature over the North Atlantic (Figure 4b), sea ice extent (Figure 5b), and deep convection (Figure 6b) are all quite similar compared to those in the original HR experiment.

Buoyancy flux correction in HR\_XRbuoy induces a drop in AMOC to roughly 14 Sv in the first 30 years but recovers soon after to about 16 Sv (magenta line in Figure 1). Since freshwater flux differences have negligible effect on the AMOC (cyan line in Figure 1), this drop is likely attributed to the lack of heat loss during winter over the North Atlantic imposed by the XR surface heat flux (Figure 3b). The coupled system has to adjust to this imposed lack of heat loss, whereby convection weakened in the initial decades in HR\_XRbuoy (Figure 7a) and likely resulted to the initial decline of the AMOC (Figure 1). While convection weakened in

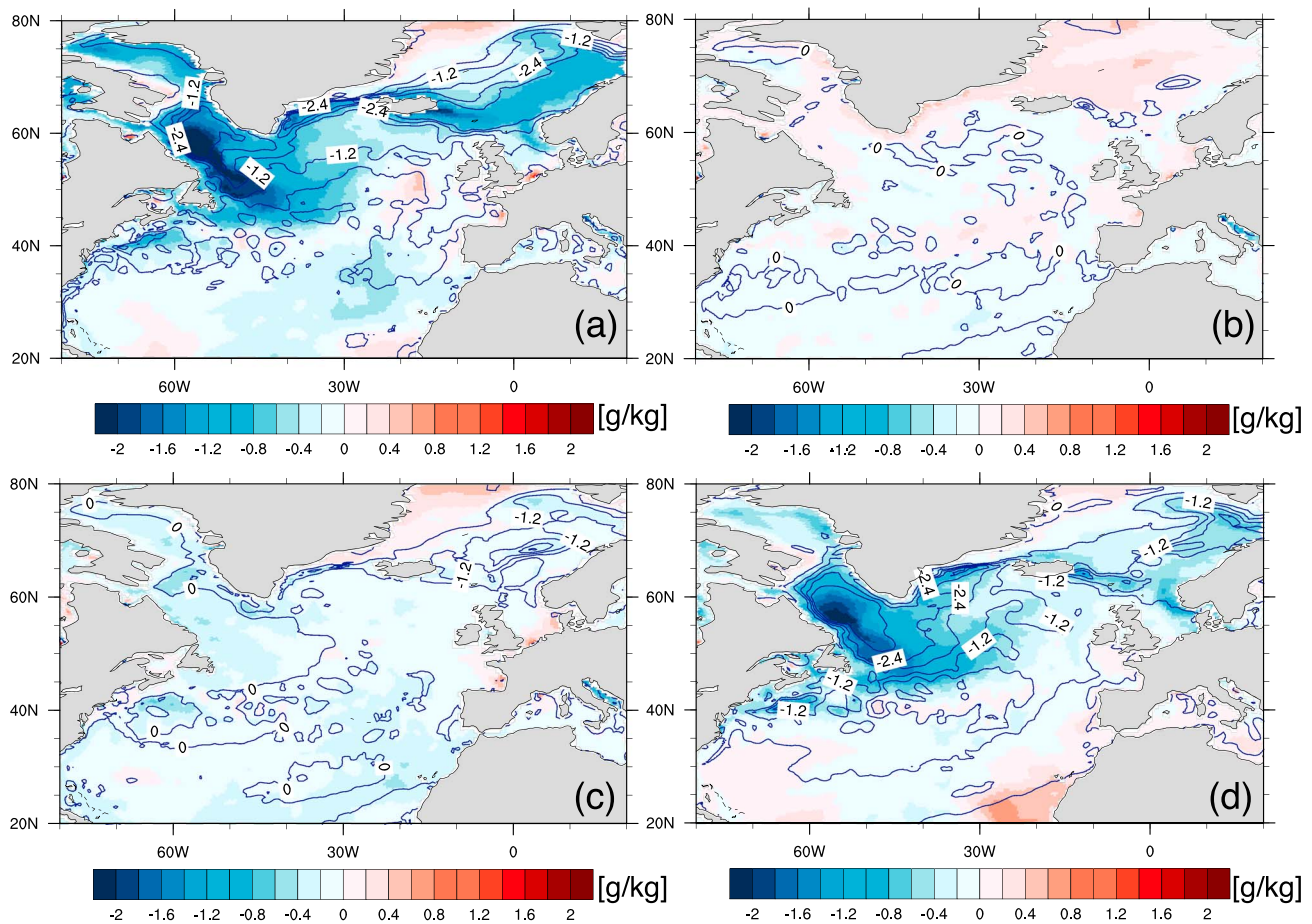


**Figure 4.** Mean difference of sea surface salinity (psu) in color and sea surface temperature (contours at 0.6 °C interval) for the first 20 years for (a) HR\_XRallflux – HRorig, (b) HR\_XRfreshwater – HRorig, (c) HR\_XRbuoy – HRorig, and (d) HR\_XRwind – HRorig.

the initial decades (20-year mean MLD over Labrador Sea of  $\sim 750$  m in HR\_XRbuoy compared to  $\sim 1,250$  m in HRorig), it did not cease like in HR\_XRwind (Figure 7a). A possible explanation is that this heat loss effect might be compensated indirectly by the stronger surface winds in HR. Since the buoyancy-corrected run leaves the wind stress unchanged, the strong wind-induced lateral transport of warm and saline subtropical North Atlantic water in HR contributes to a much weaker freshening over the North Atlantic (Figure 4c), prevents the Labrador Sea from freezing over (Figure 5c), and sustains deep water formation (Figure 6c).

Wind stress correction in HR\_XRwind induces a drop in the AMOC to almost 12 Sv in the first 40 years and slowly stabilizes around 14 Sv (green line in Figure 1). This drop is larger than those found in experiments HR\_XRfreshwater and HR\_XRbuoy. The weaker wind stress leads to weaker lateral advection of warm and saline waters from the subtropical gyre, which substantially cools and freshens the subpolar North Atlantic (Figure 4d), promotes sea ice formation (Figure 5d), and weakens deep convection in the Labrador Sea (Figure 6d). In comparison to freshwater and buoyancy effects, the dynamical wind effect dominates the freshening over the subpolar North Atlantic (Figure 4), leading to comparatively weaker deep convection (Figure 6) and greater drop in the AMOC (Figure 1).

It is worth pointing out that in our experiment setup, using a 20-year mean as a correction removes seasonality, which means that the effect of buoyancy fluxes through heat fluxes on convection is dampened. Applying seasonality to the heat flux correction translates to prescribing a forcing that would always cool surface water over the Labrador Sea via heat loss in winter, effectively overestimating the impact of heat flux and by extension, buoyancy flux (HR\_XRbuoy). However, our aim is to test how the background mean condition can be corrected for greater likeliness for convection rather than providing the driver for Labrador Sea convection through seasonal cycle. Similarly, this would be the case for wind stress that has a seasonality, indicating

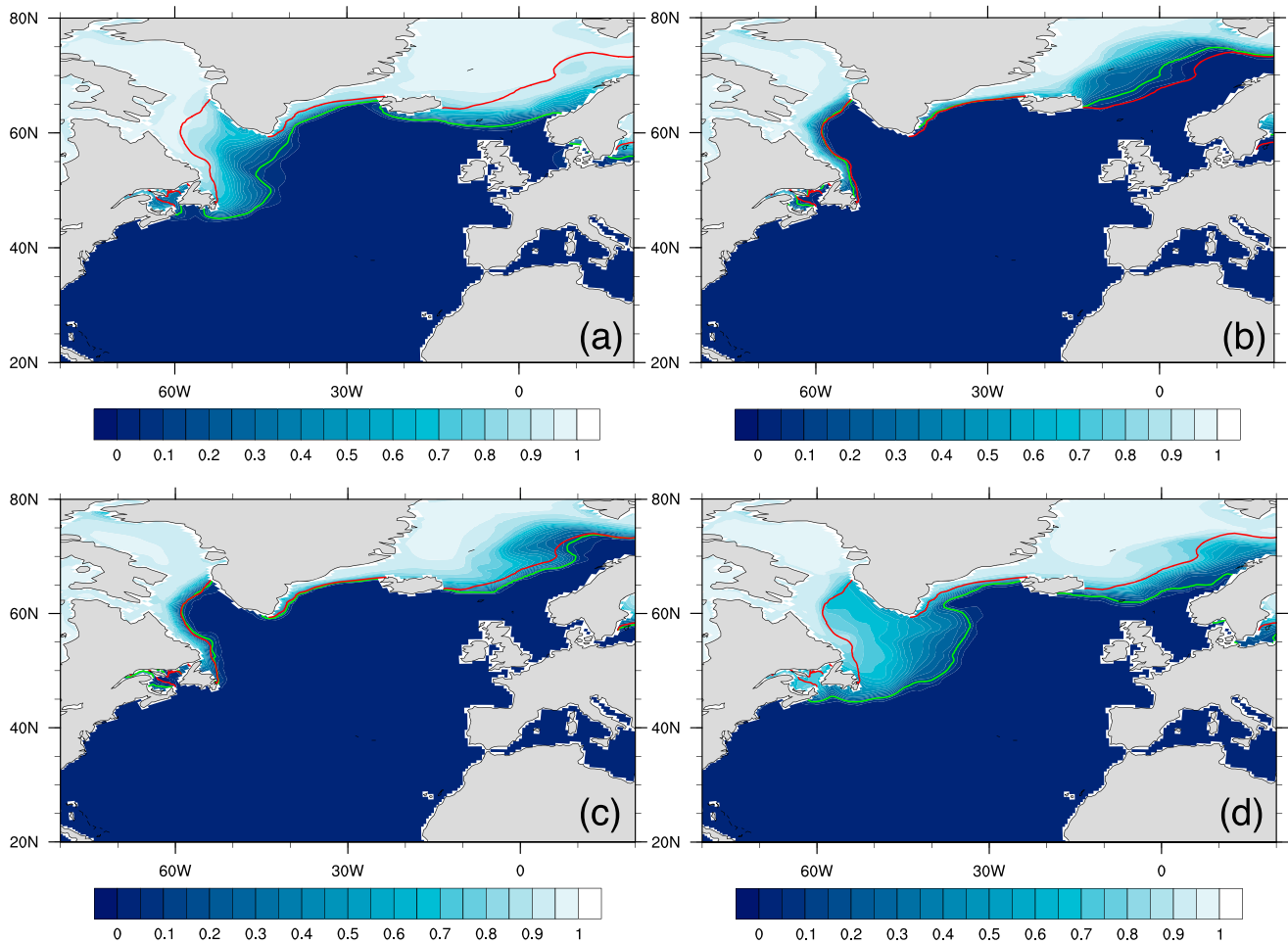


**Figure 5.** In color, mean sea ice fraction in March for the second decade of (a) HR\_XRallflux, (b) HR\_XRfreshwater, (c) HR\_XRbuoy, and (d) HR\_XRwind. Red line represents the extent of 0.15 sea ice fraction for HRorig and green line for the respective cases.

that we are also underestimating the effect of winds when we remove its seasonality (HR\_XRwind). Therefore, we opted to remove seasonality and use a 20-year mean as a background mean for our flux correction experiments. However, to ensure that impact of seasonal cycle has not been severely underestimated, we performed an additional experiment for the buoyancy flux correction that included seasonal climatology (HR\_XRbuoy\_yrmon). We found that deep convection over the Labrador Sea is very similar to HR\_XRbuoy (Figure 7a), as with the initial decline and subsequent recovery of the AMOC (Figure 1). Since there is negligible difference on the impact of using background mean flux correction in comparison to climatological seasonal flux correction, we use the background mean flux correction experiments to deduce the dominant role of wind stress over the effects of freshwater and buoyancy fluxes on the decline of the AMOC.

### 3.3. How Does Wind Stress Affect the AMOC?

The result shown in section 3.2 appears counterintuitive at first glance, given that many previous studies indicate negligible contributions of wind to a decline in AMOC (Dixon et al., 1999; Gregory et al., 2005). In addition, the salinity-advection feedback is expected to play the dominant role in the freshening of the western subpolar North Atlantic and the subsequent decline of the AMOC in XR. This section shows that the result found in section 3.2 is actually not counterintuitive. The freshening over Labrador Sea and south of Greenland can result from different processes. It can be induced directly via local surface freshwater and heat fluxes. It can also be instigated indirectly through wind-induced changes in subpolar gyre (SPG) circulation. The latter mechanism is discussed in the following.

In HRorig, similar to the AMOC strength, the SPG strength over the western North Atlantic, characterized by averaging the barotropic stream function,  $\psi_{\text{barotropic}}$ , over the area 40–60°W, 50–65°N, is stable (black line in

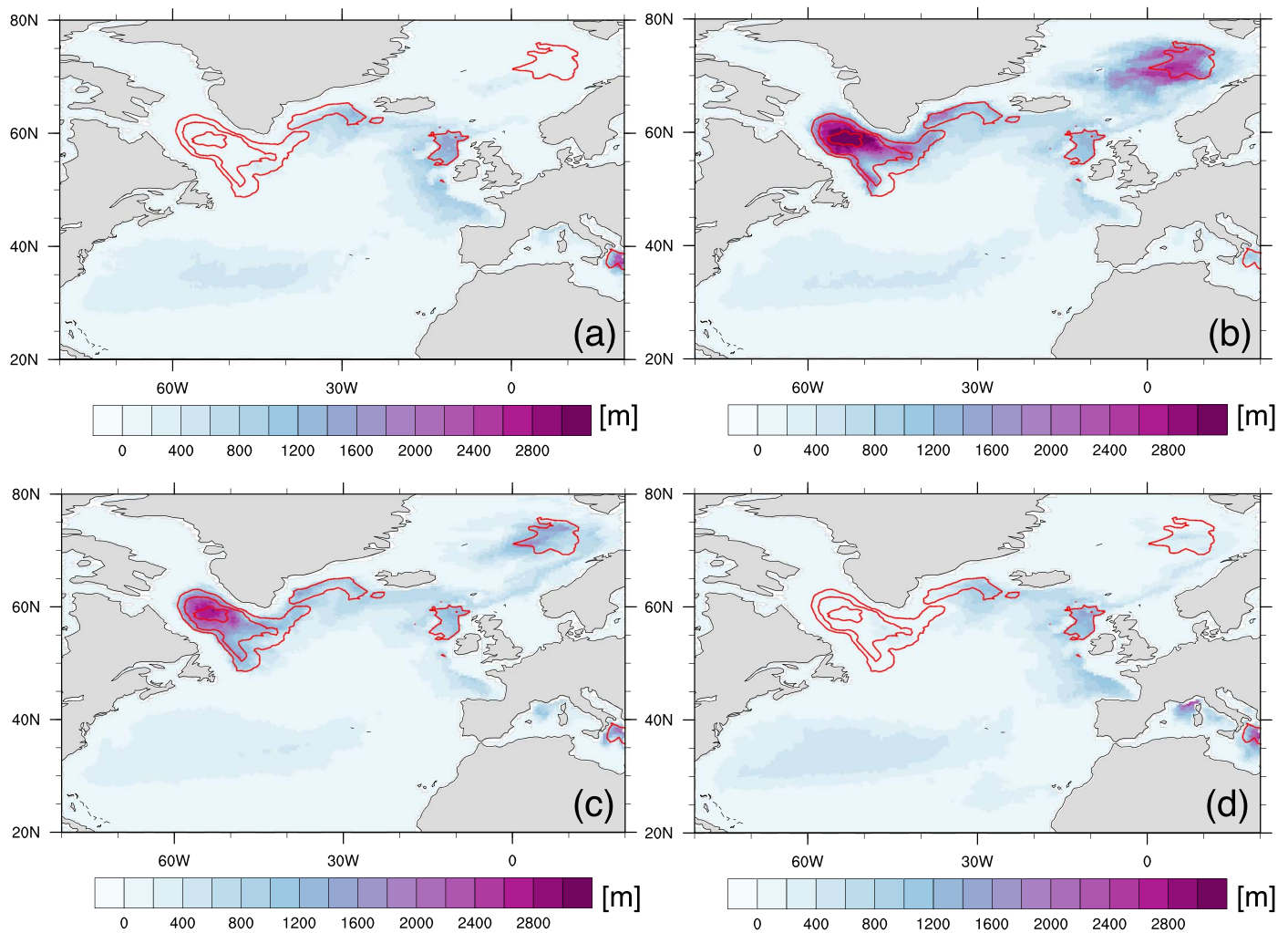


**Figure 6.** In color, mean mixed layer depth (m) in March for the second decade of (a) HR\_XRallflux, (b) HR\_XRfreshwater, (c) HR\_XRbuoy, and (d) HR\_XRwind. Red lines are 1,000-, 2,000-, and 3,000-m mixed layer depth contours from HRorig.

Figure 7b) with a mean of about 13 Sv, albeit with large variability. In XRorig, associated with the slowdown of AMOC, an immediate weakening of the western North Atlantic SPG is seen within the first 5 years (blue line in Figure 7b), which can be attributed to the dynamical effects of reduced winds. Compared to HRorig, XRorig has a weaker mean SPG strength of about 11 Sv. Surface wind stress over the subpolar North Atlantic is also much weaker in XRorig compared to HRorig (Figure 3c). The weakening is large scale, characterized by reduction of wind stress related to trades over the tropical and subtropical oceans and westerlies over the mid-latitude oceans. This meridional structure implies decreased wind stress curl, especially around 50–65°N in the North Atlantic (Figure 7c), which leads to a reduction in the wind-driven component of the North Atlantic gyre circulation.

In particular, the initial drop in overall SPG strength in XRorig can be attributed to a decrease in the wind-driven component. We compute the circulation attributable to the winds as the area average of the 2-D wind-driven stream function over the same region,  $\psi_{wind}$ . The 2-D wind-driven stream function is computed as the Sverdrup transport that is defined by the wind stress curl divided by the  $\beta$ -parameter, then zonally integrated from the east coast of the North Atlantic to its west. The difference in the 100-year mean  $\psi_{wind}$  between XRorig and HRorig amounts to about 33% loss, an approximately 3-Sv drop (red markers in Figure 7b). This value is of similar magnitude as the initial drop in the overall strength of the SPG in XRorig (blue time series in Figure 7b; note that XRorig is initialized from the same HRorig ocean state). This result indicates that the initial weakening of the SPG in XRorig can largely be explained by the weaker surface wind stress, rather than by differences in the buoyancy fluxes affecting the density component of the gyre

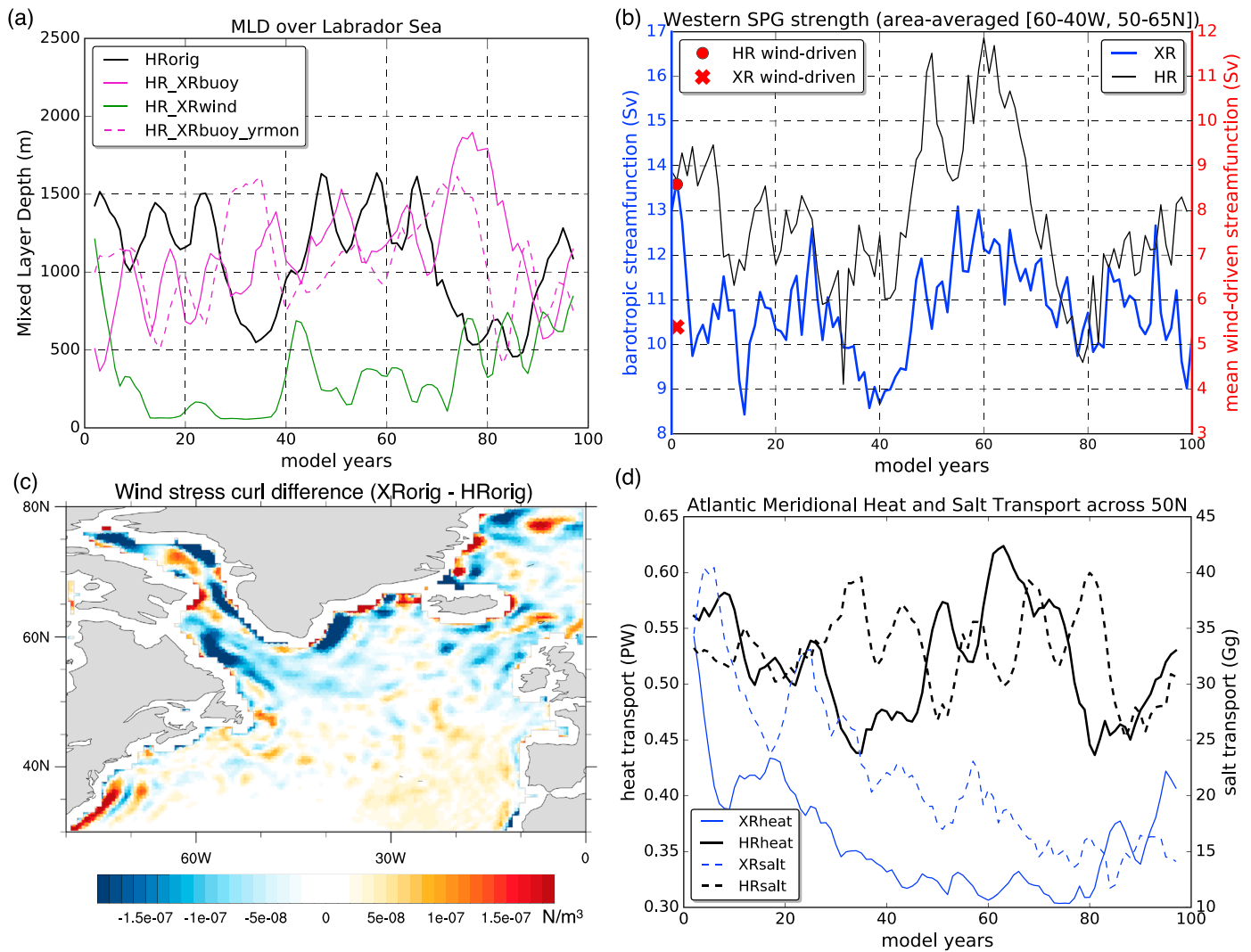


**Figure 7.** (a) Five-year running mean of mixed layer depth (m) averaged over the Labrador Sea (60–40°W, 50–65°N). (b) Time series of subpolar gyre strength defined as area-averaged barotropic stream function (Sv) over region 60–40°W, 50–65°N and multiplied by (–1); 100-year mean wind-driven gyre component for HR (red circle) and XR (red cross). (c) Mean difference of the first 20 years of (XRorig – HRorig) in the wind stress curl (N/m<sup>3</sup>). (d) Time series of meridional heat and salt transport across 50°N in the Atlantic (PW and Gg/s, respectively).

circulation. It should be noted that besides the wind-driven component of the SPG, local wind stress curl can also have an impact on the AMOC. The difference in local wind stress curl over the Labrador Sea between XRorig and HRorig (Figure 7c) indicates an anticyclonic circulation anomaly in XRorig and is associated with flattening of the isopycnals, which can weaken convection and thus the AMOC. The response of Labrador Sea convection to local wind stress curl is usually expected to be immediate. However, we see a delayed 5-year response of the deep convection to the weaker wind stress imposed in HR\_XRwind (not shown), which suggests that the weaker large-scale advection of temperature and salinity associated with the weaker SPG is the dominant contributor to the slowdown of the AMOC.

The proposed mechanistic route to explain the decline in the AMOC seen in XRorig is summarized in a schematic diagram (Figure 8). It illustrates that while local freshwater input or lack of heat loss may contribute to the weakening of the AMOC, it is momentum fluxes that is the dominant contributor to the salinity-advection feedback and decline of the AMOC. Weaker winds found in XRorig reduce the Sverdrup transport and thus weaken the SPG. The weaker SPG subsequently reduces salt and heat transport into the subpolar North Atlantic and further into the Labrador Sea. This is clearly seen in the reduction of the northward heat transport across 50°N in XRorig, which decreases to about two thirds of HRorig (Figure 7d). A

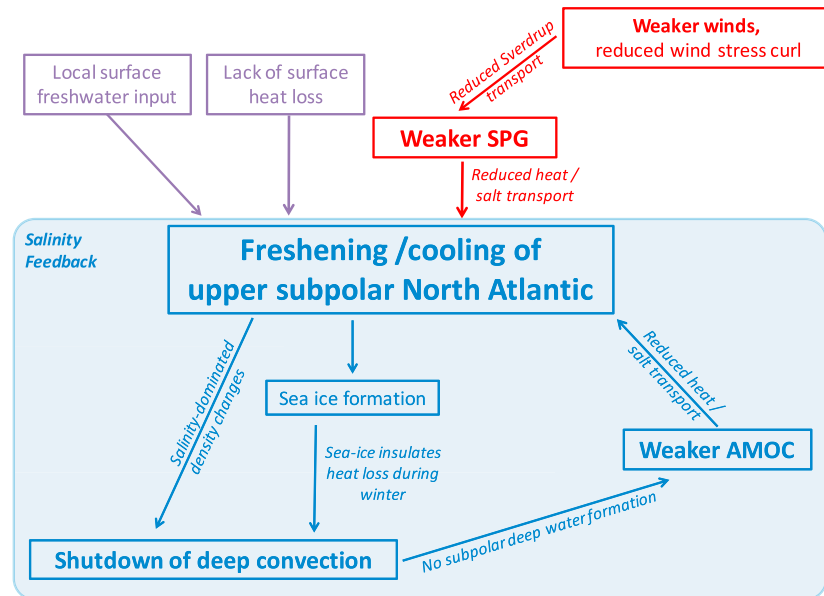


**Figure 8.** Proposed mechanistic route for the slowdown of the AMOC in XR. AMOC = Atlantic Meridional Overturning Circulation; SPG = subpolar gyre.

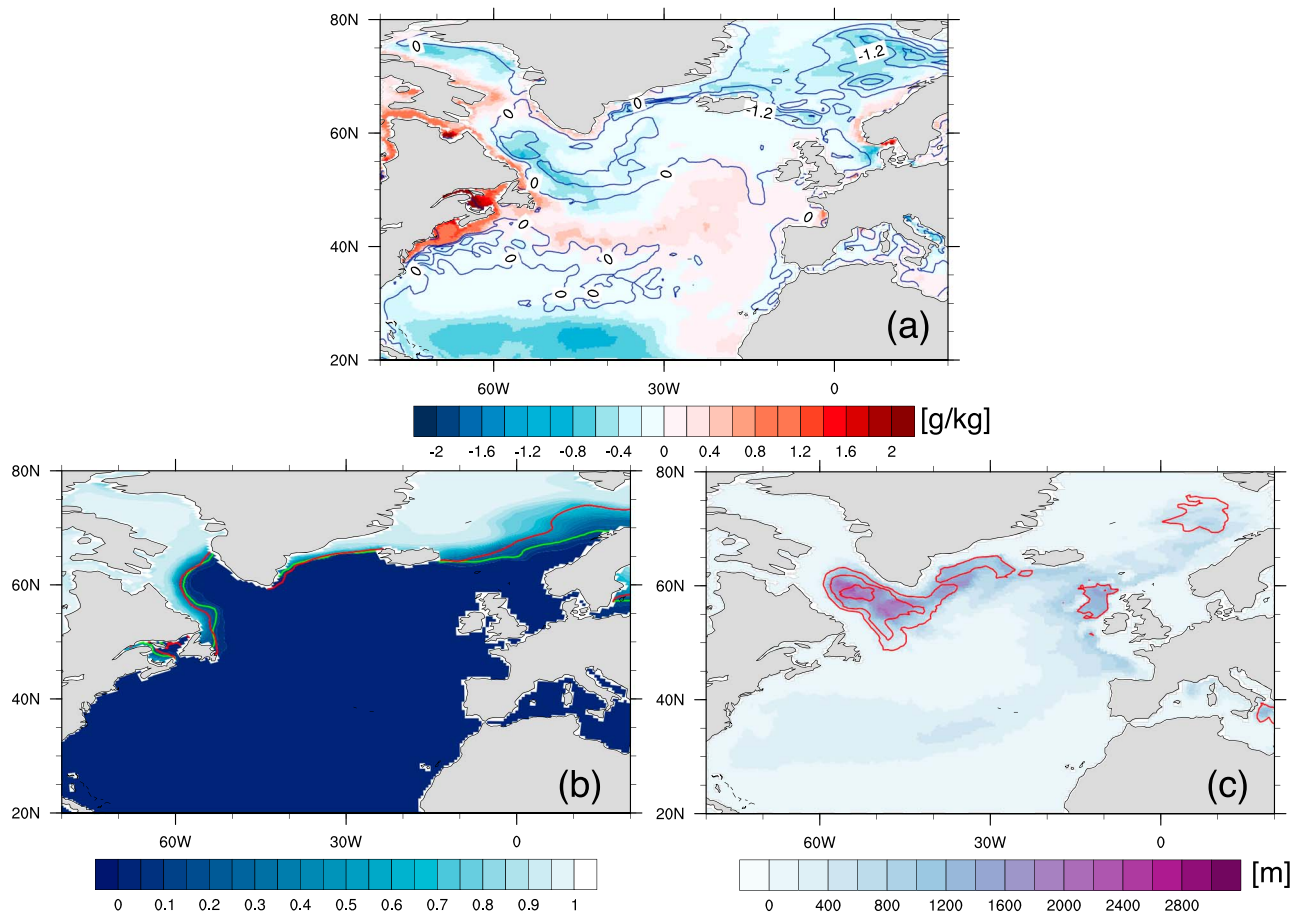


**Figure 9.** (a) Mean difference of the first 20 years of (XR\_1.5winds – HRorig) for sea surface salinity (psu) in color and sea surface temperature (contours at 0.6 °C interval). (b) Mean sea ice fraction in March for the second decade of XR\_1.5winds in color. Red line represents the extent of 0.15 sea ice fraction for HRorig and green line for XR\_1.5winds. (c) Mean mixed layer depth (m) in March for the second decade of XR\_1.5winds in color. Red lines are 1,000-, 2,000-, and 3,000-m mixed layer depth contours from HRorig.

marked reduction to about half its original value in salt transport across 50°N is seen in XRorig (Figure 7d). As a consequence of weaker gyre transport, a substantial freshening and cooling of the subpolar North Atlantic is found in XRorig compared to HRorig (Figure 2c), especially in the western part. The difference in sea surface salinity and sea surface temperature in the Labrador Sea between XRorig and HRorig can amount to 2 psu and 3 °C, respectively. Since variations in surface density in the Labrador Sea are dominated by salinity anomalies in our model simulations, surface density and thus deep convection are reduced in XRorig compared to HRorig. The freshening and cooling also primes the region for sea ice formation (Figure 2a), which when formed, insulates the surface water from heat loss during winter, leading to a complete cessation of subpolar deep convection (Figure 2b) and thus weakening the AMOC. A weakened AMOC further reduces northward salt and heat transport, providing a positive salinity-advection feedback that reinforces freshening in the subpolar North Atlantic, reduction in deep convection, and weakening of the AMOC, thereby preventing any AMOC recovery.

A further confirmation that the wind stress is largely responsible for the weakening of the AMOC in XR is supported by experiment XR1.5winds, in which wind stress over water is enhanced by a factor of 1.5. A factor of 1.5 is chosen based on the key region, the subpolar North Atlantic, where the surface wind stress in XR is weaker by about two thirds compared to HR. Note that in contrast to the flux-corrected sensitivity experiments discussed in the previous section, it uses the XR configuration and thus contains no influence from HR surface fluxes. We see that freshening and cooling over the subpolar North Atlantic for XR\_1.5winds with respect to the original HR is much less than in the original XR (Figure 9a vs. Figure 2c), even though the buoyancy fluxes are kept unchanged. In addition, sea ice extent over the Labrador Sea remains low (Figure 9b) and deep water formation continues in the Labrador Sea (Figure 9c). In this experiment, the AMOC equilibrates to about 13 Sv, which is in between HRorig and XRorig (blue dashed line in Figure 1). The decrease in AMOC during the first 40 years may be in part due to adjustment of the coupled system to the stronger wind stress in XR\_1.5winds and in part but not limited to changes in overflow properties, which will shortly be discussed in the next section.

#### 4. Discussion and Summary

Many previous studies highlight the role of freshwater and buoyancy fluxes, as well as salinity-advection feedback to a slowdown of the AMOC with negligible effects of the winds because there were no large changes in surface winds in their studies (Dixon et al., 1999; Gregory et al., 2005; Manabe & Stouffer, 1999; Mikolajewicz & Voss, 2000; Rahmstorf, 1996). In our study, salinity-advection feedback is still important, but the increase in atmospheric resolution is accompanied with a substantial reduction in surface winds over the North Atlantic, which indirectly leads to a complete shutdown of deep convection in the Labrador Sea. This is in agreement with other studies that show a large drop in surface wind stress can slow down the AMOC (Klockmann et al., 2016; Zhang et al., 2014). While winds play a big role, there are other possible factors which can potentially contribute to the AMOC decline seen in XR and will be briefly discussed here.

A key element of the complete shutdown of deep convection in the Labrador Sea in XR is the freshening of the subpolar North Atlantic. We have discussed contributions from increased surface freshwater input, as well as from reduced advection of salt from the subtropical North Atlantic. Another possible contribution is the advection of fresh water from the Arctic, mainly by the East Greenland Current. Time series of the freshwater transport through Denmark Strait, however, suggest similar mean transports in HR and XR (not shown), indicating that freshwater advection from the Arctic does not play a role in the decline of AMOC in XR.

In addition to deep convection over the Labrador Sea and entrainment of overflow waters along the way to the Labrador Sea, overflow water masses from the Nordic Seas constitute about one third of the AMOC strength in MPI-ESM, which is in agreement with Dickson and Brown (1994). We have calculated both volume transport and density of the Denmark Strait and Faroe-Shetland Channel overflow, defining the overflow as the outflow from the Nordic Seas below a depth of 400 m in Denmark Strait and 700 m in Faroe-Shetland Channel. Note that this is slightly different from the classical definition of the overflows by density threshold, as it is difficult to apply here, due to strong decline in the deep densities along the Greenland-Scotland Ridge in XR compared to HR (Figure 10 for Denmark Strait). For both Denmark Strait and Faroe-Shetland-Channel overflow, the volume transports are of similar order in HR and XR (not shown). In contrast, the density of the overflow water masses in both overflow branches decreases strongly (order of

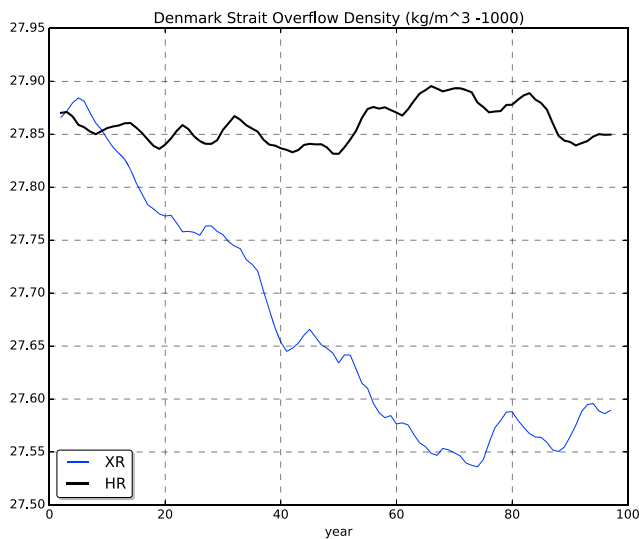


**Figure 10.** Time series of Denmark Strait overflow density ( $\text{kg/m}^3 - 1,000$ ); the overflow is defined here as outflow from the Nordic Seas below a depth of 400 m in Denmark Strait.

$0.3 \text{ kg/m}^3$ ) in XR (Figure 10 for Denmark Strait), further contributing to the AMOC decline and a shallowing of the AMOC cell. A possible explanation for the strong decrease in overflow density in XR is the shutdown of deep convection in the Nordic Seas (Figures 2b and 6a) due to the large extent of sea ice cover (Figures 2a and 5a). The latter results from strong cooling and freshening in the eastern part of the Nordic Seas (Figures 2c and 4a), in which the cooling can mainly be explained by increased surface heat loss (Figure 3b). A more detailed description of the exchanges between the Nordic Seas and the subpolar North Atlantic and their possible contribution to an AMOC decline under reduced wind forcing will be provided in a future work.

Another possible factor contributing to the AMOC decline in XR are the substantially weakened Southern Hemisphere westerlies (Figure 3c). Such weaker winds will decrease upwelling in the Southern Ocean and the strength of the return flow, which in turn may reduce the AMOC strength. We test this hypothesis by conducting a HR simulation with corrections to the wind stress in the Southern Hemisphere ( $65\text{--}45^\circ\text{S}$ ) using  $\Delta\tau = \bar{\tau}_{\text{XRorig}} - \bar{\tau}_{\text{HRorig}}$ . This is experiment HR\_XR\_SHwinds in Table 1. We find that these weaker winds have negligible effect on the AMOC decline (green dashed lines in Figure 1). Any impact of the Southern Hemisphere westerlies on the AMOC strength is likely found on longer time scales than the AMOC decline in XR, which occurs within a few decades.

The globally weaker surface winds in XR compared to HR (Figure 3c) are not necessarily expected, as one normally expects stronger winds at higher atmospheric resolution as strong winds associated with storms can be better captured at higher resolution. Comparing the three-dimensional atmospheric circulation in both resolutions, XR indeed simulates stronger tropospheric jet streams as well as a more realistic position of the jet stream over the North Atlantic (not shown). However, the surface expression of the winds in XR shows a stark reduction compared to HR. Thus, we have attempted to tune the XR atmospheric component in order to strengthen the surface winds.

Due to the higher atmospheric resolution, XR would resolve more inertial gravity waves that are otherwise not resolved but rather parameterized in HR. Hence, we have tested switching off the orographic gravity orographic wave drag and non-orographic wave drag (Hines scheme), individually and together. We have also checked the dependence of the downstream wind stress on the orographic blocking of flow by using the HR orography for drag calculations while keeping the XR orography for dynamical calculations. Unfortunately, none of these tests are able to prevent the decline of the AMOC in XR.

In another approach to strengthen the surface wind stress in XR, we tested the planetary boundary layer parameterization, particularly targeting the downward transfer of momentum. Momentum exchange between the atmospheric layers is controlled by the turbulent viscosity, which depends on the atmospheric mixing length. Thus, we have increased the mixing length from 150 m, which approximates the height of a typical atmospheric boundary layer, to a value of 300 m. We also considered momentum exchange between atmosphere and ocean that is expressed by bulk exchange formula that contains bulk transfer coefficients which depend on the surface roughness length. Over the open ocean, the roughness length is calculated after the Charnock formula and affected by the Charnock parameter, which we increased from 0.018 to 0.03, since the latter is within the bounds found in literature (Fairall et al., 1996; Garratt, 1977).

Regarding the boundary layer parameterization, especially with increasing the surface roughness length, we have been able to strengthen the surface winds on a global scale. The largest improvement is found for the Southern Hemispheric westerlies. However, with regards to the key region, the subpolar North Atlantic, none of our tuning attempts alone nor any of various combinations have yielded sufficiently strong surface winds to maintain the advection of salt and heat from the subtropics and sustain deep convection in the Labrador Sea in XR. All attempts produce a similar decline in AMOC strength. An additional attempt was made to increase the sensitivity of evaporation to winds on lower wind speed range because weaker surface winds in XR can amplify the subpolar fresh bias through the reduction of evaporation. However, this was also to no avail. While more tuning efforts of atmospheric parameters can be made to improve

AMOC strength, this would be a very expensive venture. Flux correction such as momentum or freshwater can also be implemented, but this would detract it from a freely evolving coupled climate simulation. Even though atmospheric resolution is the key issue here, changes in ocean mixing scheme that are more sensitive to winds may be beneficial. For example, some improvements in the ocean state has been seen when using the K-Profile Parameterization scheme (Large et al., 1994) compared to PP scheme by Pacanowski and Philander (1981), which is used in this work. While this is beyond the scope of this paper, we are currently investigating this as part of the model development of HighResMIP.

While the enhancement of model resolution is typically expected to provide beneficial improvements to a climate model, challenges still abound. We see that in MPI-ESM, AMOC of 17 Sv starting from an equilibrium state achieved at a lower atmospheric resolution slows down to almost half its original value when atmospheric resolution is enhanced. This decline of the AMOC is strongly related to the freshening and cooling of the Labrador Sea through the salinity-advection feedback (Figure 8). While resolution-induced differences in local heat and freshwater fluxes can contribute to the decay in AMOC, weaker surface wind stress seen in the higher-resolution simulation plays a much more prominent role, particularly the winds over the subpolar North Atlantic. These weaker winds dynamically spin down the SPG, resulting in reduced heat and salt transport from the subtropics, thereby freshening and cooling the subpolar region. This promotes sea ice formation in the Labrador Sea, and the increased presence of sea ice inhibits deep convection and deep water formation, thus slowing down the AMOC. This in turn further reduces the northward transport heat and salt and provides the positive feedback that would prevent the recovery of the AMOC. For future work, it would be of interest to evaluate the impact of enhanced ocean resolution on the AMOC.

#### Acknowledgments

This study is supported by PRIMAVERA, a Horizon 2020 project funded by the European Commission, with grant 641727. We thank the German Computing Centre (DKRZ) for providing the computational resources and the Max Planck Society for the Advancement of Science for their support. Primary data for this study are stored and made available through the Max-Planck-Gesellschaft Publications Repository ([https://pure.mpg.de/pubman/faces/ViewItemOverviewPage.jsp?itemId=item\\_3046697](https://pure.mpg.de/pubman/faces/ViewItemOverviewPage.jsp?itemId=item_3046697)). We also thank Kameswarrao Modali for providing the simulation for HRorig and Florian Ziemens for providing insightful comments and suggestions to this manuscript.

#### References

- Bond, G., Heinrich, H., Broecker, W., Labeyrie, L., McManus, J., Andrews, J., et al. (1992). Evidence for massive discharges of icebergs into the North Atlantic Ocean during the last glacial period. *Nature*, *360*, 245–249.
- Bryan, F. O., Danabasoglu, G., Nakashiki, N., Yoshida, Y., Kim, D.-H., Tsutsui, J., & Doney, S. C. (2006). Response of the North Atlantic thermohaline circulation and ventilation to increasing carbon dioxide in CCSM3. *Journal of Climate*, *19*(11), 2382–2397. <https://doi.org/10.1175/JCLI3757.1>
- Buckley, M. W., & Marshall, J. (2016). Observations, inferences, and mechanisms of the Atlantic Meridional Overturning Circulation: A review. *Reviews of Geophysics*, *54*, 5–63. <https://doi.org/10.1002/2015RG000493>
- Clark, P. U., Pisias, N. G., Stocker, T. F., & Weaver, A. J. (2002). The role of the thermohaline circulation in abrupt climate change. *Nature*, *415*, 863–869. <https://doi.org/10.1038/415863a>
- Dickson, R. R., & Brown, J. (1994). The production of North Atlantic deep water: Sources, rates, and pathways. *Journal of Geophysical Research*, *99*(C6), 12,319–12,341. <https://doi.org/10.1029/94JC00530>
- Dixon, K. W., Delworth, T. L., Spelman, M. J., & Stouffer, R. J. (1999). The influence of transient surface fluxes on North Atlantic overturning in a coupled GCM climate change experiment. *Geophysical Research Letters*, *26*(17), 2749–2752. <https://doi.org/10.1029/1999GL900571>
- Elipot, S., Frajka-Williams, E., Hughes, C. W., Olhede, S., & Lankhorst, M. (2017). Observed basin-scale response of the North Atlantic Meridional Overturning Circulation to wind stress forcing. *Journal of Climate*, *30*(6), 2029–2054. <https://doi.org/10.1175/JCLI-D-16-0664.1>
- Eyring, V., Bony, S., Meehl, G. A., Senior, C. A., Stevens, B., Stouffer, R. J., & Taylor, K. E. (2016). Overview of the Coupled Model Intercomparison Project Phase 6 (CMIP6) experimental design and organization. *Geoscientific Model Development*, *9*(5), 1937–1958. <https://doi.org/10.5194/gmd-9-1937-2016>
- Ezer, T. (2015). Detecting changes in the transport of the gulf stream and the Atlantic overturning circulation from coastal sea level data: The extreme decline in 2009–2010 and estimated variations for 1935–2012. *Global and Planetary Change*, *129*, 23–36. <https://doi.org/10.1016/j.gloplacha.2015.03.002>
- Fairall, C. W., Bradley, E. F., Rogers, D. P., Edson, J. B., & Young, G. S. (1996). Bulk parameterization of air-sea fluxes for Tropical Ocean-Global Atmosphere Coupled-Ocean Atmosphere Response Experiment. *Journal of Geophysical Research*, *101*(C2), 3747–3764. <https://doi.org/10.1029/95JC03205>
- Garratt, J. R. (1977). Review of drag coefficients over oceans and continents. *Monthly Weather Review*, *105*(7), 915–929. [https://doi.org/10.1175/1520-0493\(1977\)105<0915:RODCOO>2.0.CO;2](https://doi.org/10.1175/1520-0493(1977)105<0915:RODCOO>2.0.CO;2)
- Gent, P. R. (2018). A commentary on the Atlantic Meridional Overturning Circulation stability in climate models. *Ocean Modelling*, *122*, 57–66. <https://doi.org/10.1016/j.ocemod.2017.12.006>
- Gregory, J. M., Bouttes, N., Griffies, S. M., Haak, H., Hurlin, W. J., Jungclaus, J., et al. (2016). The Flux-Anomaly-Forced Model Intercomparison Project (FAFMIP) contribution to CMIP6: Investigation of sea-level and ocean climate change in response to CO<sub>2</sub> forcing. *Geoscientific Model Development*, *9*(11), 3993–4017. <https://doi.org/10.5194/gmd-9-3993-2016>
- Gregory, J. M., Dixon, K. W., Stouffer, R. J., Weaver, A. J., Driesschaert, E., Eby, M., et al. (2005). A model intercomparison of changes in the Atlantic thermohaline circulation in response to increasing atmospheric CO<sub>2</sub> concentration. *Geophysical Research Letters*, *32*, L12703. <https://doi.org/10.1029/2005GL023209>
- Haarsma, R. J., Roberts, M. J., Vidale, P. L., Senior, C. A., Bellucci, A., Bao, Q., et al. (2016). High Resolution Model Intercomparison Project (HighResMIP v1.0) for CMIP6. *Geoscientific Model Development*, *9*(11), 4185–4208. <https://doi.org/10.5194/gmd-9-4185-2016>
- Ilyina, T., Six, K. D., Segschneider, J., Maier-Reimer, E., Li, H., & Nez-Riboni, I. (2013). Global ocean biogeochemistry model HAMOC: Model architecture and performance as component of the MPI-Earth system model in different CMIP5 experimental realizations. *Journal of Advances in Modeling Earth Systems*, *5*, 287–315. [https://doi.org/10.1029/2012MS000178@10.1002/\(ISSN\)1942-2466.MPIESM1](https://doi.org/10.1029/2012MS000178@10.1002/(ISSN)1942-2466.MPIESM1)

- Jungclauss, J. H., Fischer, N., Haak, H., Lohmann, K., Marotzke, J., Matei, D., et al. (2013). Characteristics of the ocean simulations in the Max Planck Institute Ocean Model (MPIOM) the ocean component of the MPI-Earth system model. *Journal of Advances in Modeling Earth Systems*, 5, 422–446. <https://doi.org/10.1002/jame.20023>@10.1002/(ISSN)1942-2466.MPIESM1
- Katsman, C. A., Drijfhout, S. S., Dijkstra, H. A., & Spall, M. A. (2018). Sinking of dense North Atlantic waters in a global ocean model: Location and controls. *Journal of Geophysical Research: Oceans*, 123, 3563–3576. <https://doi.org/10.1029/2017JC013329>
- Klockmann, M., Mikolajewicz, U., & Marotzke, J. (2016). The effect of greenhouse gas concentrations and ice sheets on the glacial AMOC in a coupled climate model. *Climate of the Past*, 12(9), 1829–1846. <https://doi.org/10.5194/cp-12-1829-2016>
- Kuhlbrodt, T., Griesel, A., Montoya, M., Levermann, A., Hofmann, M., & Rahmstorf, S. (2007). On the driving processes of the Atlantic Meridional Overturning Circulation. *Reviews of Geophysics*, 45, RG2001. <https://doi.org/10.1029/2004RG000166>
- Large, W. G., McWilliams, J. C., & Doney, S. C. (1994). Oceanic vertical mixing: A review and a model with a nonlocal boundary layer parameterization. *Reviews of Geophysics*, 32(4), 363–403. <https://doi.org/10.1029/94RG01872>
- Manabe, S., & Stouffer, R. J. (1999). Are two modes of thermohaline circulation stable? *Tellus A*, 51(3), 400–411. <https://doi.org/10.1034/j.1600-0870.1999.t01-3-00005.x>
- Mauritsen, T., Stevens, B., Roeckner, E., Crueger, T., Esch, M., Giorgetta, M., et al. (2012). Tuning the climate of a global model. *Journal of Advances in Modeling Earth Systems*, 4, M00A01. <https://doi.org/10.1029/2012MS000154>
- Mecking, J. V., Drijfhout, S. S., Jackson, L. C., & Graham, T. (2016). Stable AMOC off state in an eddy-permitting coupled climate model. *Climate Dynamics*, 47(7), 2455–2470. <https://doi.org/10.1007/s00382-016-2975-0>
- Menary, M. B., Hodson, D. L. R., Robson, J. I., Sutton, R. T., Wood, R. A., & Hunt, J. A. (2015). Exploring the impact of CMIP5 model biases on the simulation of North Atlantic decadal variability. *Geophysical Research Letters*, 42, 5926–5934. <https://doi.org/10.1002/2015GL064360>
- Mikolajewicz, U., & Voss, R. (2000). The role of the individual air-sea flux components in CO<sub>2</sub>-induced changes of the ocean's circulation and climate. *Climate Dynamics*, 16(8), 627–642. <https://doi.org/10.1007/s003820000066>
- Müller, W. A., Jungclauss, J. H., Mauritsen, T., Baehr, J., Bittner, M., Budich, R., et al. (2018). A high-resolution version of the Max Planck Institute Earth System Model (MPI-ESM1.2-HR). *Journal of Advances in Modeling Earth Systems*, 10, 1383–1413. <https://doi.org/10.1029/2017MS001217>
- Pacanowski, R. C., & Philander, S. G. H. (1981). Parameterization of vertical mixing in numerical models of tropical oceans. *Journal of Physical Oceanography*, 11(11), 1443–1451. [https://doi.org/10.1175/1520-0485\(1981\)011<1443:POVMIN>2.0.CO;2](https://doi.org/10.1175/1520-0485(1981)011<1443:POVMIN>2.0.CO;2)
- Pohlmann, H., Botzet, M., Latif, M., Roesch, A., Wild, M., & Tschuck, P. (2004). Estimating the decadal predictability of a coupled AOGCM. *Journal of Climate*, 17(22), 4463–4472. <https://doi.org/10.1175/3209.1>
- Polo, I., Robson, J., Sutton, R., & Balmaseda, M. A. (2014). The importance of wind and buoyancy forcing for the boundary density variations and the geostrophic component of the AMOC at 26n. *Journal of Physical Oceanography*, 44(9), 2387–2408. <https://doi.org/10.1175/JPO-D-13-0264.1>
- Rahmstorf, S. (1996). On the freshwater forcing and transport of the Atlantic thermohaline circulation. *Climate Dynamics*, 12(12), 799–811. <https://doi.org/10.1007/s003820050144>
- Rahmstorf, S., Crucifix, M., Ganopolski, A., Goosse, H., Kamenkovich, I., Knutti, R., et al. (2005). Thermohaline circulation hysteresis: A model intercomparison. *Geophysical Research Letters*, 32, L23605. <https://doi.org/10.1029/2005GL023655>
- Reick, C. H., Raddatz, T., Brovkin, V., & Gayler, V. (2013). Representation of natural and anthropogenic land cover change in MPI-ESM. *Journal of Advances in Modeling Earth Systems*, 5, 459–482. <https://doi.org/10.1002/jame.20022>
- Roberts, C. D., Waters, J., Peterson, K. A., Palmer, M. D., McCarthy, G. D., Frajka-Williams, E., et al. (2013). Atmosphere drives recent interannual variability of the Atlantic Meridional Overturning Circulation at 26.5n. *Geophysical Research Letters*, 40, 5164–5170. <https://doi.org/10.1002/grl.50930>
- Stevens, B., Giorgetta, M., Esch, M., Mauritsen, T., Crueger, T., Rast, S., et al. (2013). Atmospheric component of the MPIM Earth system model: ECHAM6. *Journal of Advances in Modeling Earth Systems*, 5, 146–172. <https://doi.org/10.1002/jame.20015>
- Stommel, H. (1961). Thermohaline convection with two stable regimes of flow. *Tellus*, 13(2), 224–230. <https://doi.org/10.1111/j.2153-3490.1961.tb00079.x>
- Taylor, K. E., Stouffer, R. J., & Meehl, G. A. (2012). An overview of CMIP5 and the experiment design. *Bulletin of the American Meteorological Society*, 93(4), 485–498. <https://doi.org/10.1175/BAMS-D-11-00094.1>
- Valcke, S. (2013). The OASIS3 coupler: A European climate modelling community software. *Geoscientific Model Development*, 6(2), 373–388. <https://doi.org/10.5194/gmd-6-373-2013>
- Weijer, W., Maltrud, M. E., Hecht, M. W., Dijkstra, H. A., & Kliphuis, M. A. (2012b). Response of the Atlantic Ocean circulation to Greenland ice sheet melting in a strongly eddying ocean model. *Geophysical Research Letters*, 39, L09606. <https://doi.org/10.1029/2012GL051611>
- Weijer, W., Sloyan, B. M., Maltrud, M. E., Jeffery, N., Hecht, M. W., Hartin, C. A., et al. (2012a). The Southern Ocean and its climate in CCSM4. *Journal of Climate*, 25(8), 2652–2675. <https://doi.org/10.1175/JCLI-D-11-00302.1>
- Zhang, X., Lohmann, G., Knorr, G., & Purcell, C. (2014). Abrupt glacial climate shifts controlled by ice sheet changes. *Nature*, 512, 290–294.
- Zhao, J., & Johns, W. (2014). Wind-forced interannual variability of the Atlantic Meridional Overturning Circulation at 26.5n. *Journal of Geophysical Research: Oceans*, 119, 2403–2419. <https://doi.org/10.1002/2013JC009407>